

CBNetV2: A Composite Backbone Network Architecture for Object Detection

Tingting Liang*, Xiaojie Chu*, Yudong Liu*, Yongtao Wang, Zhi Tang, Wei Chu, Jingdong Chen, Haibin Ling

Abstract—Modern top-performing object detectors depend heavily on backbone networks, whose advances bring consistent performance gains through exploring more effective network structures. In this paper, we propose a novel and flexible backbone framework, namely *CBNetV2*, to construct high-performance detectors using *existing* open-sourced pre-trained backbones under the pre-training fine-tuning paradigm. In particular, CBNetV2 architecture groups multiple identical backbones, which are connected through composite connections. Specifically, it integrates the high- and low-level features of multiple backbone networks and gradually expands the receptive field to more efficiently perform object detection. We also propose a better training strategy with *assistant supervision* for CBNet-based detectors. CBNetV2 has strong generalization capabilities for different backbones and head designs of the detector architecture. Without additional pre-training of the composite backbone, CBNetV2 can be adapted to various backbones (*i.e.*, CNN-based vs. Transformer-based) and head designs of most mainstream detectors (*i.e.*, one-stage vs. two-stage, anchor-based vs. anchor-free-based). Experiments provide strong evidence that, compared with simply increasing the depth and width of the network, CBNetV2 introduces a more efficient, effective, and resource-friendly way to build high-performance backbone networks. Particularly, our Dual-Swin-L achieves 59.4% box AP and 51.6% mask AP on COCO *test-dev* under the single-model and single-scale testing protocol, which is significantly better than the state-of-the-art result (*i.e.*, 57.7% box AP and 50.2% mask AP) achieved by Swin-L, while the training schedule is reduced by 6 \times . With multi-scale testing, we push the current best single model result to a new record of 60.1% box AP and 52.3% mask AP without using extra training data. Code is available at <https://github.com/VDIGPKU/CBNetV2>.

Index Terms—Deep Learning, Object Detection, Backbone Networks, Composite Architectures.

1 INTRODUCTION

OBJECT detection is one of the fundamental problems in computer vision, serving a wide range of applications such as autonomous driving, intelligent video surveillance, remote sensing, *etc.* In recent years, great progresses have been made for object detection thanks to the booming development of deep convolutional networks [2], and excellent detectors have been proposed, *e.g.*, SSD [3], YOLO [4], Faster R-CNN [5], RetinaNet [6], ATSS [7], Mask R-CNN [8], Cascade R-CNN [9], *etc.*

Typically, in a Neural Network (NN)-based detector, a backbone network is used to extract basic features for detecting objects, and usually designed originally for image classification and pre-trained on the ImageNet dataset [10]. Intuitively, the more representative features extracted by the backbone, the better the performance of its host detector. To obtain higher accuracy, deeper and wider backbones have been exploited by mainstream detectors (*i.e.*, from mobile-size models [11], [12] and ResNet [13], to ResNeXt [14] and Res2Net [15]). Recently, Transformer [16] based backbones have also been explored and have shown very promising performance. Overall, advances in large backbone pre-training demonstrate a trend towards more effective and efficient multi-scale representations in object detection.

Encouraged by the results achieved by pre-trained large backbone-based detectors, we seek further improvement to construct high-performance detectors by exploiting existing well-designed backbone architectures and their pre-trained weights. Though one may design a new improved backbone, the expertise and computing resources overhead can be expensive. On the one hand, designing a new architecture of backbone requires expert experience and a lot of trial and error. On the other hand, pre-training a new backbone (especially for large models) on ImageNet requires a large amount of computational resource, which makes it costly to obtain better detection performance following pre-training and fine-tuning paradigm. Alternatively, training detectors from scratch saves the cost of pre-training, but requires even more computing resources and training skills to train the detector [17].

In this paper, we present a simple and novel composition approach to use existing pre-trained backbones under the pre-training fine-tuning paradigm. Unlike most previous methods that focus on modular crafting and require pre-training on ImageNet to strengthen the representation, we improve the existing backbone representation ability without additional pre-training. As shown in Fig. 1, our solution, named *Composite Backbone Network V2* (CBNetV2), groups multiple identical backbones together. Specifically, parallel backbones (named assisting backbones and lead backbone) are connected via *composite connections*. From left to right in Fig. 1, the output of each stage in an assisting backbone flows to the parallel and lower-level stages of its succeeding sibling. Finally, the features of the lead backbone are fed to the neck and detection head for bounding box regression and classification. Contrary to simple network deepening or widening, CBNetV2 integrates the high- and low-level features of multiple

- Corresponding author: Yongtao Wang. * indicates equal contribution.
- T. Liang, X. Chu, Y. Liu, Y. Wang, Z. Tang are with the Wangxuan Institute of Computer Technology, Peking University, Beijing 100080, China. E-mail: {tingtingliang, bahuangliuhe, wyt, tangzhi}@pku.edu.cn, chuxiaojie@stu.pku.edu.cn
- W. Chu, J. Cheng are with Data and Platform Technology Devision of Ant Group, China. E-mail: {weichu.cw, jingdongchen.cjd}@antgroup.com
- H. Ling is with the Department of Computer Science, Stony Brook University, Stony Brook, NY 11794, USA. E-mail: hling@cs.stonybrook.edu.
- A preliminary version of this manuscript was published in [1].

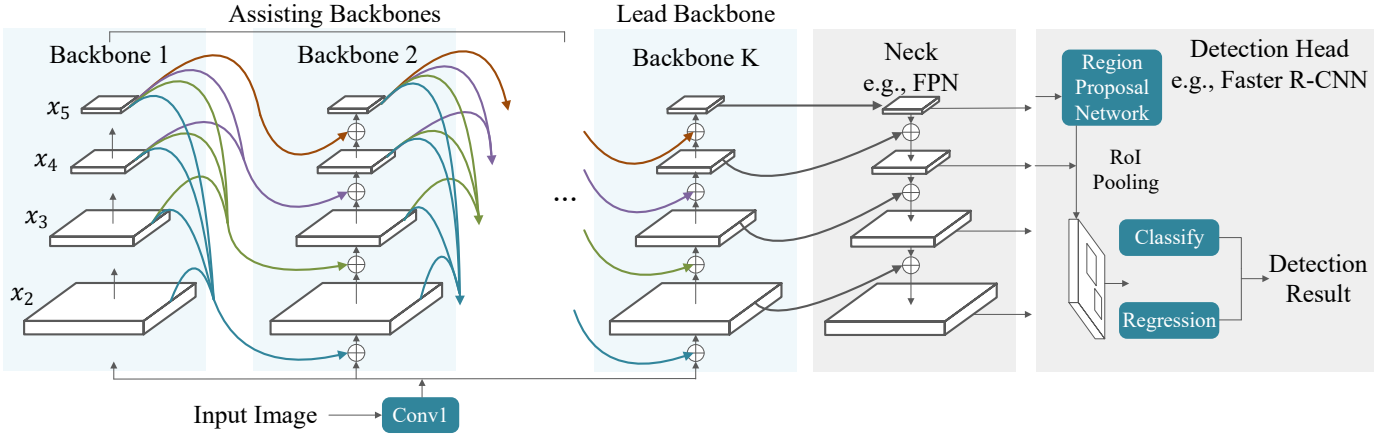


Fig. 1. Illustration of the proposed Composite Backbone Network V2 (CBNetV2) architecture for object detection.

backbone networks and progressively expands the receptive field for more efficient object detection. Notably, each assembled backbone of CBNetV2 is *initialized by the weights of an existing open source pre-trained individual backbone* (e.g., Dual-ResNet50¹ is initialized by the weights of ResNet50 [13], which are available in the open source community). In addition, to further exploit the potential of CBNetV2, we propose an effective training strategy with supervision for assisting backbones, achieving higher detection accuracy than the original CBNet [1] while not sacrificing inference speed.

We demonstrate the effectiveness of our framework by conducting experiments on the challenging MS COCO benchmark [18]. Experiments show that CBNetV2 has strong generalization capabilities for different backbones and head designs of the detector architecture, which enables us to train detectors that significantly outperform detectors based on larger backbones. Specifically, CBNetV2 can be applied to various backbones (e.g., from convolution-based [13], [14], [15] to Transformer-based [19]). Compared to the original backbones, our Dual-Backbone boosts their performance by 3.4%~3.5% AP, demonstrating the effectiveness of the proposed CBNetV2. At comparable model complexity, our Dual-Backbone still improves by 1.1% ~ 2.1% AP, indicating that the composed backbone is more efficient than the pre-trained wider and deeper network. Moreover, CBNetV2 can be flexibly plugged into mainstream detectors (e.g., RetinaNet [6], ATSS [7], Faster R-CNN [5], Mask R-CNN [8], Cascade R-CNN and Cascade Mask R-CNN [9]), and consistently improve the performances of these detectors by 3%~3.8% AP, demonstrating its strong adaptability to various head designs of detectors. Remarkably, our CBNetV2 presents a general and resource-friendly framework to drive the accuracy ceiling of high-performance detectors. Without bells and whistles, our Dual-Swin-L achieves unparalleled single-model single-scale result of 59.4% box AP and 51.6% mask AP on COCO *test-dev*, surpassing the state-of-the-art result (i.e., 57.7% box AP and 50.2% mask AP obtained by Swin-L), while reducing the training schedule by 6×. With multi-scale testing, we push the current best single-model result to a new record of 60.1% box AP and 52.3% mask AP.

The main contributions of this paper are listed as follows:

- We propose a general, efficient and effective framework,

1. Here and after, Dual-Backbone (DB) and Triple-Backbone (TB) respectively represent consisting of 2 and 3 identical backbones.

CBNetV2 (Composite Backbone Network V2), to construct high-performance backbone networks for object detection without additional pre-training.

- We propose Dense Higher-Level Composition (DHLC) style and assistant supervision to more efficiently use existing pre-trained weights for object detection under pre-training fine-tuning paradigm.
- Our Dual-Swin-L achieves a new record of single-model single-scale result on COCO at a shorter (by 6×) training schedule than Swin-L. With multi-scale testing, our method achieves the best known result without extra training data.

2 RELATED WORK

Object Detection. Object detection aims to locate each object instance from a predefined set of classes in an input image. With the rapid development of convolutional neural networks (CNNs), there is a popular paradigm for deep learning-based object detectors: the backbone network (typically designed for classification and pre-trained on ImageNet) extracts basic features from the input image, and then the neck (e.g., feature pyramid network [21]) enhances the multi-scale features from the backbone, after which the detection head predicts the object bounding boxes with position and classification information. Based on detection heads, the cutting edge methods for generic object detection can be briefly categorized into two major branches. The first branch contains one-stage detectors such as YOLO [4], SSD [3], RetinaNet [6], NAS-FPN [22], and EfficientDet [23]. The other branch contains two-stage methods such as Faster R-CNN [5], FPN [21], Mask R-CNN [8], Cascade R-CNN [9], and Libra R-CNN [24]. Recently, academic attention has been geared toward anchor-free detectors due partly to the emergence of FPN [21] and focal Loss [6], where more elegant end-to-end detectors have been proposed. On the one hand, FSAF [25], FCOS [26], ATSS [7] and GFL [27] improve RetinaNet with center-based anchor-free methods. On the other hand, CornerNet [28] and CenterNet [29] detect object bounding boxes with a keypoint-based method.

More recently, Neural Architecture Search (NAS) is applied to automatically search the architecture for a specific detector. NAS-FPN [22], NAS-FCOS [30] and SpineNet [31] use reinforcement learning to control the architecture sampling and obtain promising results. SM-NAS [32] uses evolutionary algorithm and

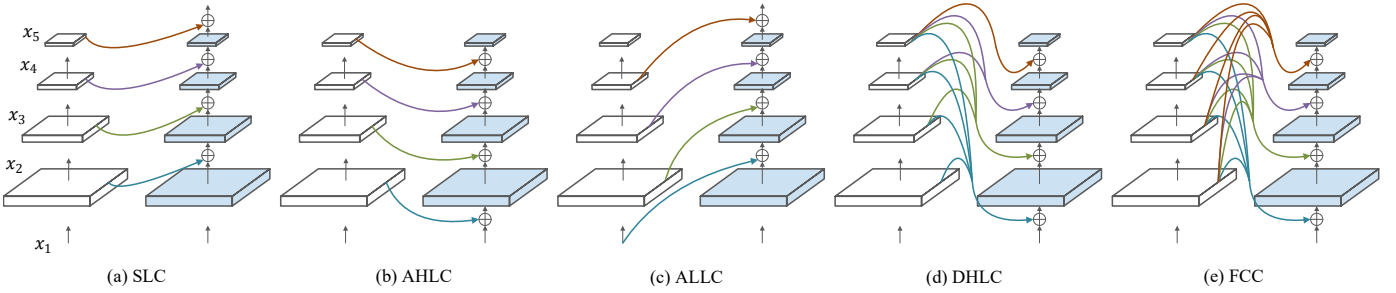


Fig. 2. Five kinds of composite styles for Dual-Backbone architecture (an assisting backbone and a lead backbone). (a) Same Level Composition (SLC). (b) Adjacent Higher-Level Composition (AHLC). (c) Adjacent Lower-Level Composition (ALLC). (d) Dense Higher-Level Composition (DHLC). (e) Full-connected Composition (FCC). The composite connection are colored lines representing some operations such as element-wise operation, scaling, 1×1 Conv layer and BN layer.

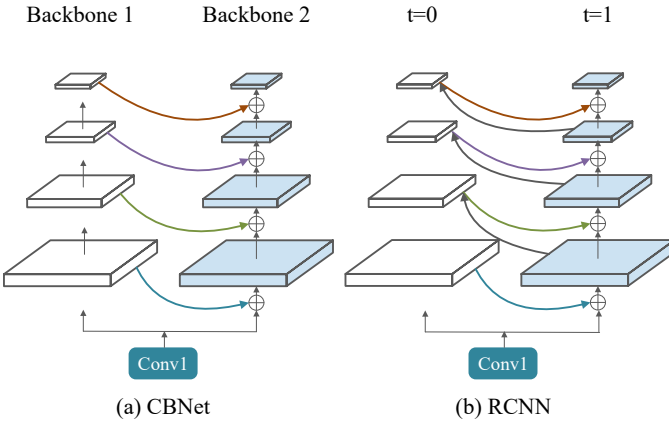


Fig. 3. Comparison between our proposed CBNet architecture ($K = 2$) and the unrolled architecture of RCNN [$T = 2$].

partial order pruning method to search the optimal combination of different parts of the detector. Auto-FPN [33] uses the gradient-based method to search for the best detector. DetNAS [34] and OPANAS [35] use the one-shot method to search for an efficient backbone and neck for object detection, respectively.

In addition to the above CNN-based detectors, Transformer [16] has also been utilized for detection. DETR [36] proposes a fully end-to-end detector by combining CNN and Transformer encoder-decoders. Swin Transformer [19] proposes a general-purpose Transformer backbone to reduce computational complexity and has been a tremendous success in object detection.

Backbone for Object Detection. Starting from AlexNet [2], deeper and wider backbones have been exploited by mainstream detectors, such as VGG [37], ResNet [13], DenseNet [38], ResNeXt [14], and Res2Net [15]. Since the backbone network is usually designed for classification, whether it is pre-trained on ImageNet and fine-tuned on a given detection dataset or trained from scratch on the detection dataset, it requires many computational resources and is difficult to optimize. Recently, two non-trivially designed backbones, *i.e.*, DetNet [39] and FishNet [40], are specifically designed for the detection task. However, they still require pre-training for classification tasks before fine-tuning on detection task. Res2Net [15] achieves impressive results in object detection by representing multi-scale features at the granular level and increasing the range of receptive fields for each network layer. In addition to manually designing the backbone architecture, DetNAS [34] uses NAS to search for a better back-

bone for object detection, thereby reducing the cost of manual design. Swin Transformer [19] utilizes Transformer modular to build the backbone and achieves impressive results, despite the need of expensive pre-training.

It is well known that designing and pre-training a new and robust backbone requires significant computational costs. Alternatively, we propose a more economical and efficient solution to build a more powerful object detection backbone, by assembling multiple identical existing backbones (*e.g.*, ResNet [13], ResNeXt [14], Res2Net [15], and Swin Transformer [19]).

Recurrent Convolution Neural Network. Different from the feed-forward architecture of CNN, Recurrent CNN (RCNN) [20] incorporates recurrent connections into each convolution layer. This property enhances the ability of the model to integrate contextual information, which is important for object recognition. As shown in Fig. 3, our proposed Composite Backbone Network shares some similarities with the unfolded RCNN [20], but they are very different. First, as shown in Fig. 3, the connections between the parallel stages in CBNet are unidirectional, but they are bidirectional in RCNN. Second, in RCNN, the parallel stages at different time steps share parameter weights, while in the proposed CBNet, the parallel stages of backbones are independent of each other. Moreover, we need to pre-train RCNN on ImageNet if we use it as the backbone of the detector. By contrast, CBNet does not require additional pre-training because it directly uses existing pre-trained weights.

3 PROPOSED METHOD

This section elaborates the proposed CBNetV2 in details. In Sec. 3.1 and Sec. 3.2, we describe its basic architecture and variants, respectively. In Sec. 3.3, we propose a training strategy for CBNet-based detectors. In Sec. 3.4, we briefly introduce the pruning strategy. In Sec. 3.5, we summarize the detection framework of CBNetV2.

3.1 Architecture of CBNetV2

The proposed CBNetV2 consists of K identical backbones ($K \geq 2$). In particular, we call the case $K = 2$ (shown in Fig. 3.a) as **Dual-Backbone (DB)**, and the case $K=3$ as **Triple-Backbone (TB)**.

As illustrated in Fig. 1, the CBNetV2 architecture includes two types of backbones: lead backbone B_K and assisting backbones B_1, B_2, \dots, B_{K-1} . Each backbone comprises L stages (usually $L = 5$), and each stage consists of several convolutional layers

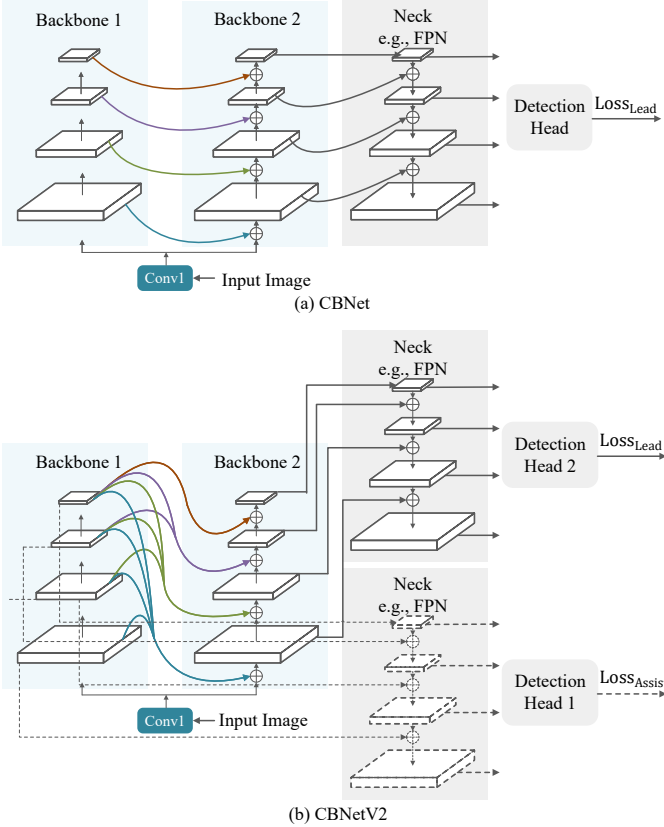


Fig. 4. (a) CBNet [1] ($K=2$). (b) CBNetV2 ($K=2$) with assistant supervision. The two FPNs and detection heads share the same weights. It is worth noting that the main differences between CBNetV2 and its previous version are in composite styles and training strategies.

with feature maps of the same size. The l -th stage of the backbone implements the non-linear transformation $F^l(\cdot)$ ($l = 1, 2, \dots, L$).

Most conventional convolutional networks follow the design of encoding the input images into intermediate features with monotonically decreased resolution. In particular, the l -th stage takes the output (denoted as x^{l-1}) of the previous ($l-1$)-th stage as input, which can be expressed as follows:

$$x^l = F^l(x^{l-1}), l \geq 2. \quad (1)$$

Differently, we adopt assisting backbones B_1, B_2, \dots, B_{K-1} to improve the representative ability of lead backbone B_K . We iterate the features of a backbone to its successor in a stage-by-stage fashion. Thus, Equation (1) can be rewritten as:

$$x_k^l = F_k^l(x_k^{l-1} + g^{l-1}(x_{k-1})), l \geq 2, k = 2, 3, \dots, K, \quad (2)$$

where $g^{l-1}(\cdot)$ represents the composite connection, which takes features (denoted as $x_{k-1} = \{x_{k-1}^i | i = 1, 2, \dots, L\}$) from assisting backbone B_{k-1} as input and takes the features of the same size as x_k^{l-1} as output. Therefore, the output features of B_{k-1} are transformed and contribute to the input of each stage in B_k . Note that $x_1^1, x_2^1, \dots, x_K^1$ are weight sharing.

For the object detection task, only the output features of the lead backbone $\{x_K^i, i = 2, 3, \dots, L\}$ are fed into the neck and then the RPN/detection head, while the outputs of the assisting backbone are forwarded to its succeeding siblings. It is worth noting that B_1, B_2, \dots, B_{K-1} can be used for various backbone architectures (e.g., ResNet [13], ResNeXt [14], Res2Net [15],

and Swin Transformer [19]) and initialized directly from the pre-trained weights of a single backbone.

3.2 Possible Composite Styles

For the composite connection $g^l(x)$, which takes $x = \{x^i | i = 1, 2, \dots, L\}$ from an assisting backbone as input and outputs a feature of the same size of x^l (omitting k for simplicity), we propose the following five different composite styles.

3.2.1 Same Level Composition (SLC)

An intuitive and simple way of compositing is to fuse the output features from the same stage of backbones. As shown in Fig. 2.a, the operation of Same Level Composite (SLC) can be formulated as:

$$g^l(x) = \mathbf{w}(x^l), l \geq 2, \quad (3)$$

where \mathbf{w} represents a 1×1 convolution layer and a batch normalization layer.

3.2.2 Adjacent Higher-Level Composition (AHLC)

Motivated by Feature Pyramid Networks [21], the top-down pathway introduces the spatially coarser, but semantically stronger, higher-level features to enhance the lower-level features of the bottom-up pathway. In the previous CBNet [1], we conduct the Adjacent Higher-Level Composition (AHLC) to feed the output of the adjacent higher-level stage of the previous backbone to the subsequent one (from left to right in Fig. 2.b):

$$g^l(x) = \mathbf{U}(\mathbf{w}(x^{l+1})), l \geq 1, \quad (4)$$

where $\mathbf{U}(\cdot)$ indicates the up-sampling operation.

3.2.3 Adjacent Lower-Level Composition (ALLC)

Contrary to AHLC, we introduce a bottom-up pathway to feed the output of the adjacent lower-level stage of the previous backbone to the succeeding one. This operation of Adjacent Lower-Level Composition (ALLC) is shown in Fig. 2.c, which is formulated as:

$$g^l(x) = \mathbf{D}(\mathbf{w}(x^{l-1})), l \geq 2, \quad (5)$$

where $\mathbf{D}(\cdot)$ denotes the down-sample operation.

3.2.4 Dense Higher-Level Composition (DHLC)

In DenseNet [38], each layer is connected to all subsequent layers to build comprehensive features. Inspired by this, we utilize dense composite connections in our CBNet architecture. The operation of DHLC is expressed as follows:

$$g^l(x) = \sum_{i=l+1}^L \mathbf{U}(\mathbf{w}_i(x^i)), l \geq 1. \quad (6)$$

As shown in Fig. 2.d, when $K = 2$, we compose the features from all the higher-level stages in the previous backbone and add them to the lower-level stages in the latter one.

3.2.5 Full-connected Composition (FCC)

As shown in Fig. 2.e, we compose features from all the stages in the previous backbones and feed them to each stage in the following one. Compared to DHLC, we add connections in low-high-level case. The operation of FCC can be expressed as:

$$g^l(x) = \sum_{i=2}^L \mathbf{I}(\mathbf{w}_i(x^i)), l \geq 1, \quad (7)$$

where $\mathbf{I}(\cdot)$ denotes scale-resizing, $\mathbf{I}(\cdot) = \mathbf{D}(\cdot)$ when $i > l$, and $\mathbf{I}(\cdot) = \mathbf{U}(\cdot)$ when $i < l$.

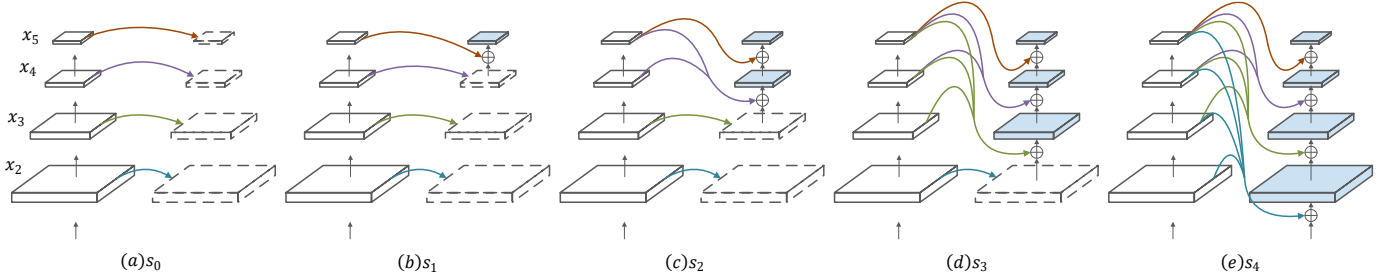


Fig. 5. Illustration of different pruning strategies for dual-backbone. s_i denotes that there are i stages $\{x_{6-i}, x_{7-i}, \dots, x_5 | i = 0, 1, 2, 3, 4\}$ in lead backbone.

3.3 Assistant Supervision

Although increasing the depth usually leads to performance improvement [13], it may introduce additional optimization difficulties, as in the case of image classification [41]. The studies in [42], [43] introduce the auxiliary classifiers of intermediate layers to improve the convergence of very deep networks. In original CBNNet, although the composite backbones are parallel, the latter backbone (*e.g.*, lead backbone in Fig. 4.a) deepen the network through adjacent connections between the previous backbone (*e.g.*, assisting backbone in Fig. 4.a). To better train the CBNNet-based detector, We propose to generate initial results of assisting backbones by supervision with the auxiliary neck and detection head to provide additional regularization.

An example of our supervised CBNNetV2 when $K=2$ is illustrated in Fig. 4.b. Apart from the original loss that uses lead backbone feature to train the detection head 1, another detection head 2 takes assisting backbone features as input, producing *assistant supervision*. Note that detection head 1 and detection head 2 are weight sharing, as are the two necks. The assistant supervision helps to optimize the learning process, while the original loss for the lead backbone takes the greatest responsibility. We add weights to balance the assistant supervision, where the total loss is defined as:

$$\mathcal{L} = \mathcal{L}_{\text{Lead}} + \sum_{i=1}^{K-1} (\lambda_i \cdot \mathcal{L}_{\text{Assist}}^i). \quad (8)$$

where $\mathcal{L}_{\text{Lead}}$ is the loss of lead backbone, $\mathcal{L}_{\text{Assist}}^i$ is the loss of assisting backbones, and λ_i is the loss weight for the i -th assisting backbone.

During the inference phase, we abandon the assistant supervision branch and only utilize the output features of lead backbone in CBNNetV2 (Fig. 4.b). Consequently, assistant supervision does not affect the inference speed.

3.4 Pruning Strategy for CBNNetV2

To reduce the model complexity of CBNNetV2, we explore the possibility of pruning different number of stages in 2, 3, ..., K -th backbones instead of composing the backbones in a holistic manner (*i.e.*, adding identical backbones to the original one). For simplicity, we show the case when $K = 2$ in Fig. 5. There are five ways to prune the lead backbone. s_i indicates there are i stages ($\{x_{6-i}, x_{7-i}, \dots, x_5 | i = 0, 1, 2, 3, 4\}$) in the lead backbone and the pruned stages are filled by the features of the same stages in the first backbone. Details can be found in Sec. 4.4.4.

3.5 Architecture of Detection Network with CBNNetV2

The CBNNetV2 can be applied to various off-the-shelf detectors without additional modifications to the network architecture. In practice, we attach the lead backbone with functional networks, *e.g.*, FPN [21] and detection head. The inference phase of CBNNetV2 for object detection is shown in Fig. 1.

4 EXPERIMENTS

In this section, we evaluate our proposed approach through extensive experiments. In Sec. 4.1, we detail the experimental setup. In Sec. 4.2, we compare our method with state-of-the-art detection methods. In Sec. 4.3, we demonstrate the generality of our method by performing experiments on different backbones and detectors. In Sec. 4.4, we conduct an extensive ablation study and analysis to investigate individual components of our framework. Finally we visualize some qualitative results of our proposed method in Sec. 4.5.

4.1 Implementation details

4.1.1 Datasets and Evaluation Criteria

We conduct experiments on the COCO [18] benchmark. The training is conducted on the 118k training images, and ablation studies on the 5k minival images. We also report the results on the 20k images in *test-dev* for comparison with the state-of-the-art (SOTA) methods. For evaluation, we adopt the metrics from the COCO detection evaluation criteria, including the mean Average Precision (AP) across IoU thresholds ranging from 0.5 to 0.95 at different scales.

4.1.2 Training and Inference Details

Our experiments are based on the open source detection toolbox MMDetection [48]. For ablation studies and simple comparisons, we resize input size to 800×500 during training and inference if not specified. We choose Faster R-CNN (ResNet50 [13]) with FPN [21] as the baseline. We use the SGD optimizer with an initial learning rate of 0.02, momentum of 0.9, and 10^{-4} as weight decay. We train detectors for 12 epochs with learning rate decreased by $10\times$ at epoch 8 and 11. We use only random flip for data augmentation and set the batch size to 16. Note that experiments related to Swin Transformer that are not highlighted specifically follow the hyper-parameters of [19]. The inference speed FPS (Frames per second) for detector is measured on a machine with 1 V100 GPU.

To compare with state-of-the-art detectors, we utilize multi-scale training [49] (the short side resized to $400 \sim 1400$ and the long side is at most 1600) and longer training schedule (details

TABLE 1

Comparison with the state-of-the-art object detection results on the COCO *test-dev* set. Our Dual-Res2Net101-DCN achieves new state-of-the-art bbox AP over previous anchor-free-based and anchor-based detectors while using comparable or fewer training epochs.

	Method	AP ^{box}	AP ^{box} ₅₀	AP ^{box} ₇₅	AP ^{box} _S	AP ^{box} _M	AP ^{box} _L	Params	Epochs
<i>anchor-free-based</i>	FSAF [25]	42.9	63.8	46.3	26.6	46.2	52.7	94 M	24
	FCOS [26]	44.7	64.1	48.4	27.6	47.5	55.6	90 M	24
	DETR-DC5 [36]	44.9	64.7	47.7	23.7	49.5	62.3	60 M	500
	NAS-FCOS [30]	46.1	-	-	-	-	-	89 M	24
	ATSS [7]	47.7	66.5	51.9	29.7	50.8	59.4	95 M	24
	GFL [27]	48.2	67.4	52.6	29.2	51.7	60.2	53 M	24
	Deformable DETR [44]	50.1	69.7	54.6	30.6	52.8	64.7	-	50
	PAA [45]	50.8	69.7	55.1	31.4	54.7	65.2	129 M	24
	Dual-Res2Net101-DCN (ATSS)	52.7	71.1	57.7	35.7	56.6	62.7	107 M	20
<i>anchor-based</i>	Auto-FPN [33]	44.3	-	-	-	-	-	90 M	24
	SM-NAS:E5 [32]	45.9	64.6	49.6	27.1	49.0	58.0	-	24
	NAS-FPN [22]	48.3	-	-	-	-	-	-	150
	SP-NAS [46]	49.1	67.1	53.5	31	52.6	63.7	-	50
	SpineNet-190 [31]	52.1	71.8	56.5	35.4	55	63.6	164 M	250
	OPANAS [35]	52.2	71.3	57.3	33.3	55.6	65.4	83 M	24
	EfficientDet-D7x [23]	55.1	74.3	59.9	-	-	-	77 M	600
	YOLOv4-P7 [47]	55.5	73.4	60.8	38.4	59.4	67.7	288 M	450
	Dual-Res2Net101-DCN (Cascade R-CNN)	55.6	73.7	60.8	37.4	59.0	67.6	146 M	32

can be found in Sec. 4.2). During inference phase, we use SoftNMS [50] with a threshold of 0.001, and the input size is set to 1600×1400 . All other hyper-parameters in this paper follow MMDetection if not specified.

4.2 Comparison with State-of-the-Art

We compare our methods with cutting edge detectors. We divide the results into object detection (Table 1) and instance segmentation (Table 2) according to whether or not the instance segmentation annotations are used during training. Following [19], we improve the detector heads of Cascade R-CNN, Cascade Mask R-CNN, and HTC in the above two tables by adding four convolution layers [54] in each bounding box head and using GIoU loss [55] instead of Smooth L1 [56].

4.2.1 Object Detection

For detectors trained with only bounding box annotations, we summarize them into two categories: anchor-based, and anchor-free-based in Table 1. We select ATSS [7] as our anchor-free representative, and Cascade R-CNN as our anchor-based representative.

Anchor-free. Dual-Res2Net101-DCN equipped with ATSS is trained for 20 epochs, where the learning rate is decayed by $10\times$ in the 16th and 19th epochs. Notably, our Dual-Res2Net101-DCN achieves 52.8% AP, outperforming previous anchor-free methods [7], [25], [26], [27], [30], [36], [44] under single-scale testing protocol.

Anchor-based. Our Dual-Res2Net101-DCN achieves 55.6% AP, surpassing other anchor-based detectors [22], [23], [31], [32], [33], [35], [46], [57]. It is worth noting that our CBNetV2 trains only for 32 epochs (the first 20 epochs are regular training and the remaining 12 epochs are trained with Stochastic Weights Averaging [58]), being $16\times$ and $12\times$ shorter than EfficientDet and YOLOv4, respectively.

4.2.2 Instance Segmentation

We further compare our method with state-of-the-art results [19], [51], [52], [53] using both bounding box and instance

segmentation annotations in Table 2. Following [19], we provide results with the backbone pre-trained on regular ImageNet-1K and ImageNet-22K to show the high capacity of CBNetV2.

Results with regular ImageNet-1K pre-train. Following [19], 3x schedule (36 epochs with the learning rate decayed by $10\times$ at epochs 27 and 33) is used for Dual-Swin-S. Using Cascade Mask R-CNN, our Dual-Swin-S achieves 56.3% box AP and 48.6% mask AP on COCO *minival* in terms of the bounding box and instance segmentation, showing significant gains of +4.4% box AP and +3.6% mask AP to Swin-B with similar model size and the same training protocol. In addition, Dual-Swin-S achieves 56.9% box AP and 49.1% mask AP on COCO *dev*, outperforming other ImageNet-1K pre-trained backbone-based detectors.

Results with ImageNet-22K pre-train. Our Dual-Swin-B achieves single-scale result of 58.4% box AP and 50.7% mask AP on COCO *minival*, which is 1.3% box AP and 1.2% mask AP higher than that of Swin-L (HTC++) [19] while the number of parameters is decreased by 17% and the training schedule is reduced by $3.6\times$. Especially, with only 12 epochs training (which is $6\times$ shorter than Swin-L), our Dual-Swin-L achieves 59.4% box AP and 51.6% mask AP on COCO *test-dev*, outperforming prior arts. We can push the current best result to a new record of 60.1% box AP and 52.3% mask AP through multi-scale testing. These results demonstrate that our CBNetV2 proposes an efficient, effective, and resource-friendly framework to build high-performance backbone networks.

4.3 Generality of CBNetV2

CBNetV2 expands the receptive field by combining the backbones in parallel, rather than simply increasing the depth of the network. To demonstrate the effectiveness and generality of our design strategy, we perform experiments on various backbones and different head designs of the detector architecture.

4.3.1 Generality for Main-stream Backbone Architectures

Effectiveness To demonstrate the effectiveness of CBNetV2, we conduct experiments on Faster R-CNN with different backbone architectures. As shown in Table 3, for CNN-based backbones (*e.g.*,

TABLE 2

Comparison with the state-of-the-art object detection and instance segmentation results on COCO. In collaboration with Swin Transformer, our CBNetV2 achieves the state-of-the-art bbox AP and mask AP while using fewer training epochs.

Pre-trained on	Method	mini-val		test-dev		Params	Epochs
		AP ^{box}	AP ^{mask}	AP ^{box}	AP ^{mask}		
ImageNet-1K	GCNet* [51]	51.8	44.7	52.3	45.4	-	36
	Swin-B [19]	51.9	45.0	-	-	145 M	36
	ResNeSt-200* [52]	52.5	-	53.3	47.1	-	36
	CopyPaste [53] [†]	55.9	47.2	56.0	47.4	185 M	96
	Dual-Swin-S (Cascade Mask R-CNN)	56.3	48.6	56.9	49.1	156 M	36
ImageNet-22K	Swin-L (HTC++) [19]	57.1	49.5	57.7	50.2	284 M	72
	Swin-L (HTC++) [19]*	58.0	50.4	58.7	51.1	284 M	72
	Dual-Swin-B (HTC)	58.4	50.7	58.7	51.1	235 M	20
	Dual-Swin-B (HTC)*	58.9	51.3	59.3	51.8	235 M	20
	Dual-Swin-L (HTC)	59.1	51.0	59.4	51.6	453 M	12
	Dual-Swin-L (HTC)*	59.6	51.8	60.1	52.3	453 M	12

¹ * indicates method with multi-scale testing.

² † indicates additional unlabeled data are used to pretrain backbone.

TABLE 3

Comparison between Dual-Backbone (s_3 version in Fig. 6) and single backbones in terms of different architectures. Our Dual-Backbone boosts the performance of CNN-based backbones by over 3.4% AP.

Backbone	AP ^{box}		Δ AP ^{box}
	single	dual	
ResNet50	34.6	38.0	+3.4
ResNeXt50-32x4d	36.3	39.8	+3.5
Res2Net50	37.7	41.2	+3.5

ResNet, ResNeXt-32x4d, and Res2Net), our method can boost baseline by over 3.4% AP. Furthermore, CBNetV2 is not only compatible with CNN-based backbones, but also with transformer-based backbones (for details, see Sec. 4.3.2).

Efficiency Note that the number of parameters in CBNetV2 has increased compared to the baseline. To better demonstrate the efficiency of the composite architecture, we compare CBNetV2 with deeper and wider backbone networks. As shown in Table 4, with comparable number of FLOPs and inference speed, CBNetV2 improves ResNet101, ResNeXt101-32x4d, Res2Net101 by 1.7%, 2.1%, and 1.1% AP, respectively. Additionally, Dual-ResNeXt50-32x4d is 1.1% AP higher than that of ResNeXt101-64x4d, while the number of parameters is only 70%. The results demonstrate that our composite backbone architecture is more efficient and effective than simply increasing the depth and width of the network.

4.3.2 Generality for Swin Transformer

Transformer is notable for the use of attention to model long-range dependencies in data, and Swin Transformer [19] is one of the most representative recent arts. Specifically, Swin Transformer is a general-purpose Transformer backbone that constructs hierarchical feature maps and has linear computational complexity in image size. We conduct experiments on Swin Transformer to show the model generality of CBNetV2. For a fair comparison, we follow the same training strategy as [19] with multi-scale training (the short side resized to 480 ~ 800 and the long side at most 1333), AdamW optimizer (initial learning rate of 0.0001, weight decay of 0.05, and batch size of 16), and 3x schedule (36 epochs).

As shown in Table 5, the accuracy of the model slowly increases as the Swin Transformer is deepened and widened,

TABLE 4

Comparison between Dual-Backbone (s_3) and deeper and wider single backbones in terms of different architectures. The backbones in each group are sorted by FLOPs for efficiency comparison. Backbones armed with our proposed method are more efficient than their own wider and deeper version.

Backbone	AP ^{box}	Params	FLOPs	FPS
ResNet101	36.3	60.5 M	121 G	25.8
Dual-ResNet50	38.0	69.4 M	121 G	23.3
ResNet152	37.8	76.2 M	151 G	21.3
ResNeXt101-32x4d	37.7	60.2 M	122 G	20.8
Dual-ResNeXt50-32x4d	39.8	68.4 M	123 G	19.3
ResNeXt101-64x4d	38.7	99.3 M	183 G	15.8
Res2Net101	40.1	61.2 M	125 G	20.7
Dual-Res2Net50	41.2	69.7 M	125 G	20.2
Res2Net200	41.7	92.2 M	185 G	14.8

TABLE 5

Comparison between Dual-Swin-T and the single Swin equipped with Cascade Mask R-CNN. Swin-T composited by our method is more effective and efficient than its own wider and deeper version.

Backbone	AP ^{box}	AP ^{mask}	Params	FLOPs	FPS
Swin-T	50.5	43.7	85.6 M	742 G	7.8
Swin-S	51.8 ^{+1.3}	44.7 ^{+1.0}	107.0 M	832 G	7.0
Swin-B	51.9 ^{+1.4}	45.0 ^{+1.3}	145.0 M	975 G	5.9
Dual-Swin-T	53.6^{+3.1}	46.2^{+2.5}	113.8 M	836 G	6.5

and saturates at Swin-S. Swin-B is only 0.1% AP higher than that of Swin-S, but the amount of parameters increases by 38M. When using Dual-Swin-T, we achieve 53.6% box AP and 46.2% mask AP by improving Swin-T 3.1% box AP and 2.5% mask AP. Surprisingly, our Dual-Swin-T is 1.7% box AP and 1.2% mask AP higher than that of the deeper and wider Swin-B while the model complexity is lower (e.g., FLOPs 836G vs. 975G, Params 113.8M vs. 145.0M). These results prove that CBNetV2 can also improve non-pure convolutional architectures. They also demonstrate that CBNetV2 pushes the upper limit of accuracy for high-performance detectors more effectively than simply increasing the depth and width of the network.

4.3.3 Model Adaptability for Mainstream Detectors

We evaluate the adaptability of CBNetV2 by plugging it into mainstream detectors such as RetinaNet, ATSS, Faster R-CNN, Mask

TABLE 6

Comparison of ResNet50 and the proposed Dual-ResNet50 on different detectors. Our Dual-ResNet50 significantly boosts all popular object detectors by 3.0% ~ 3.8% bbox AP and 2.9% mask AP.

Detector	AP ^{box}		Δ AP ^{box}	AP ^{mask}		Δ AP ^{mask}
	single	dual		single	dual	
RetinaNet	33.2	36.2	+3.0	-	-	-
ATSS	36.9	39.9	+3.0	-	-	-
Faster R-CNN	34.6	38.1	+3.5	-	-	-
Mask R-CNN	35.2	39.0	+3.8	31.8	34.7	+2.9
Cascade R-CNN	38.2	41.2	+3.0	-	-	-

TABLE 7

Experimental results on the compatibility of CBNetV2 and deformable convolution. CBNetV2 and deformable convolution can be superimposed on each other without conflict.

Backbone	AP ^{box}		Δ AP ^{box}
	w/o DCN	w/ DCN	
ResNet50	34.6	37.4	+2.8
ResNet152	37.8	39.8	+2.0
Dual-ResNet50	38.1	40.4	+2.3
ResNeXt50-32x4d	36.3	38.6	+2.3
ResNeXt101-64x4	38.7	41.0	+2.3
Dual-ResNeXt50-32x4	39.8	42.5	+2.7

R-CNN, and Cascade R-CNN. These methods present a variety of detector head designs (*e.g.*, two-stage vs. one-stage, anchor-based vs. anchor-free). As shown in Table 6, our CBNetV2 significantly boosts all popular object detectors by over 3% AP. The instance segmentation accuracy of Mask R-CNN is also improved by 2.9% AP. These results demonstrate the robust adaptability of CBNetV2 to various head designs of detectors.

4.3.4 Compatibility of CBNetV2 with Deformable Convolution

Deformable convolution [59] enhances the transformation modeling capability of CNNs and is widely used for accurate object detectors (*e.g.*, simply adding DCN improves Faster R-CNN ResNet50 from 34.6% to 37.4% AP). To show the compatibility of our CBNetV2 architecture with deformable convolution, we perform experiments on ResNet and ResNeXt equipped with Faster R-CNN. As shown in Table 7, DCN is still effective on Dual-Backbone with 2.3% AP~2.7% AP improvement. This improvement is greater than the 2.0% AP and 1.3% AP increments on ResNet152 and ResNeXt101-64x4d. On the other hand, Dual-Backbone increases ResNet50-DCN by 3.0% AP and is 0.6% higher than that of the deeper ResNet152-DCN. In addition, Dual-Backbone increases ResNet50-32x4d-DCN by 3.7% AP, which is 1.3% higher than that of the deeper and wider ResNeXt101-64x4d-DCN. The results show that the effects of CBNetV2 and deformable convolution can be superimposed without conflicting with each other.

4.4 Ablation Studies

We ablate various design choices for our proposed CBNetV2. For simplicity, all accuracy results here are on the COCO validation set with 800×500 input size if not specified.

4.4.1 Effectiveness of Different Composite Styles

We conduct experiments to compare the proposed composite styles in Fig. 2, including SLC, AHLC, ALLC, DHLC and FCC. All

TABLE 8

Comparison between different composite styles. Obviously, DHLC achieves the best FLOPs-accuracy and Params-accuracy trade-offs.

Composite style	AP ^{box}	Params	FLOPs
-	34.6	41.5 M	90 G
SLC	35.0	64.8 M	123 G
AHLC	36.0	67.6 M	148 G
ALLC	32.4	67.6 M	156 G
DHLC	37.3	69.7 M	150 G
FCC	37.4	72.0 M	168 G

TABLE 9

Ablation study of different loss weights for assistant supervision.

# Backbones	λ_1	λ_2	AP ^{bbox}
Dual	0	-	37.3
	0.125	-	37.6
	0.25	-	37.8
	0.5	-	38.1
	1.0	-	37.9
Triple	0	0	37.4
	0.25	0.25	37.9
	0.25	0.5	38.9
	0.5	0.5	38.6
	0.5	1.0	39.2

these experiments are conducted based on the Faster R-CNN Dual-ResNet50 architecture. Results are shown in Table 8.

SLC gets a slightly better result than that of the single-backbone baseline. We speculate that this is because the features extracted by the same stage of both backbones are similar, and thus SLC can only learn a slightly more semantic information than a single backbone do.

AHLC raises the baseline by 1.4% AP, which verifies our motivation in Sec. 3.2.2, *i.e.*, if the higher-level features of the assisting backbone are fed to the lower-level stages of the lead backbone, the semantic information of the latter will be enhanced.

ALLC degrades the performance of the baseline by 2.2% AP. We infer that if we directly add the lower-level (*i.e.*, shallower) features of the assisting backbone to the higher-level (*i.e.*, deeper) ones of the lead backbone, the semantic information of the latter will be largely hurt.

DHLC improves the performance of the baseline by a large margin (from 34.6% AP to 37.3% AP by 2.7% AP). More composite connections of the high-low cases enrich the representation ability of features to some extent.

FCC achieves the best performance of 37.4% AP thanks to the fully connected architecture.

In summary, FCC and DHLC achieve the two best results. Considering the computational simplicity, we recommend using DHLC for CBNetV2. All the above composite styles have similar amount of parameters, but the accuracy varies greatly. These results prove that simply increasing the number of parameters or adding a backbone network does not guarantee better result. Therefore, composite connection is the key to compose backbones. These results show that the suggested DHLC composite style is effective and nontrivial.

4.4.2 Different Weights for Assistant Supervision

Experimental results related to weighting the assistant supervision are presented in Table 9. For simplicity, we perform DHLC composite style on CBNetV2. The first setting is the Faster R-CNN

TABLE 10
Ablation study of individual components of the proposed CBNetV2.

# Backbones	DHLC	Supervision	AP ^{bbbox}
Single			34.6
Dual	✓		36.0
		✓	37.3
	✓	✓	38.1
Triple	✓		36.4
		✓	37.4
	✓	✓	39.2

Dual-ResNet50 baseline and the second is the Triple-ResNet50 baseline, where the λ for assisting backbone in Equation (8) is set to zero. For the Dual-Backbone (DB) structure, the baseline can be improved by 0.8% AP by setting λ_1 to 0.5. For the Triple-Backbone (TB) structure, the baseline can be improved by 1.8% AP by setting $\{\lambda_1, \lambda_2\}$ to $\{0.5, 1.0\}$. The experimental results verify that the assistant supervision forms an effective training strategy that improves the performance of CBNetV2.

4.4.3 Effectiveness of Each Component

To further analyze the importance of each component in CBNetV2, composite backbone, DHLC composite style, and assistant supervision are progressively applied to the model to verify the effectiveness. We choose AHLC in CBNet [1] as default composite style.

The results are summarized in Table 10. It shows that the Dual-Backbone (DB) and Triple-Backbone (TB) improve the baseline by 1.4% and 1.8% AP, respectively. It validates the effectiveness of our composite backbone structure (CBNet [1]). The DHLC composite style further improves the detection performance of DB and TB by over 1.0% AP. The results confirm that DHLC enables a larger receptive field, with features at each level obtaining rich semantic information from all higher-level features. The assistant supervision brings about 1.0% AP increment to DB and TB, thanks to the supervision of assisting backbones forming a better training strategy and improving the representative ability of the lead backbone. Note that the assistant supervision does not introduce extra parameters during the inference phase. When combining the three components, there is a significant improvement over the baseline. The DHLC-style DB and TB with assistant supervision achieve 37.9% AP and 38.9% AP, respectively, with +3.3% AP and +4.3% AP increments. Also, CBNetV2 improves CBNet [1] by 1.8% and 1.7% AP in terms of DB and TB respectively. In brief, each component in CBNetV2 brings improvements to the detector and they are complementary to each other.

4.4.4 Efficiency of Pruning Strategy

As shown in Fig. 6, with the 78pruning strategy, our Dual-ResNet50 family and Triple-ResNet50 family achieve better FLOPs-accuracy trade-offs than ResNet family. This also illustrates the efficiency of our pruning strategy. In particular, the number of FLOPs in s_3 is reduced by 10% compared to s_4 , but the accuracy is decreased by only 0.1%. This is because the weights of the pruned stage are fixed during the detector training [48] so pruning this stage does not sacrifice detection accuracy. Hence, when speed and memory cost need to be prioritized, we suggest pruning the fixed stages in 2, 3, ..., K -th backbones in CBNetV2.

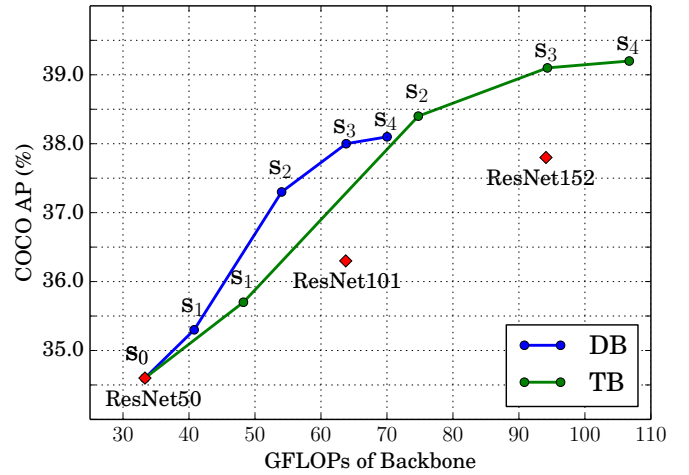


Fig. 6. Performance comparison of different pruning strategies for Dual-ResNet50 (DB) and Triple-ResNet50 (TB).

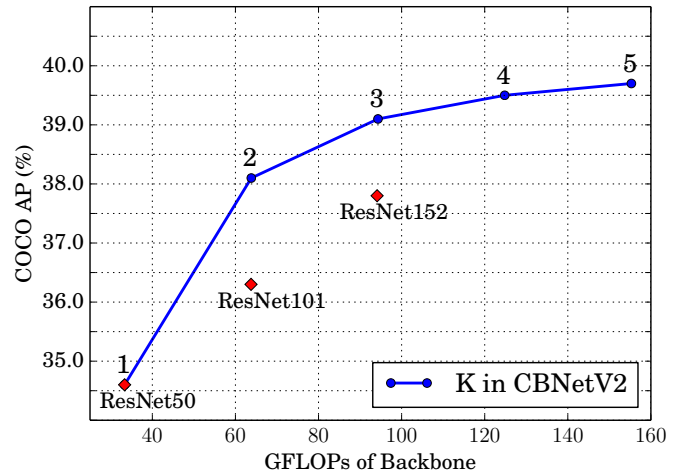


Fig. 7. Performance comparison of CBNetV2 with different numbers of composite backbones (K).

4.4.5 Effectiveness on Different Number of Backbones in CBNetV2

To further explore the ability of CBNetV2 to construct high-performance detectors, we evaluate the efficiency of our CBNetV2 (s_3 version) by controlling the number of backbones. As shown in Fig. 7, we vary the number of backbones (e.g., $K = 1, 2, 3, 4, 5$) and compare their performance and computational cost (GFLOPs) with the ResNet family. Note that the accuracy continues to increase as the complexity of the model increases. Compared with ResNet152, our method obtains higher accuracy at $K=2$ while computation cost is lower. Meanwhile, the accuracy can be further improved for $K=3, 4, 5$. CBNetV2 provides an effective and efficient alternative to improve the model performance rather than simply increasing the depth or width of the network.

4.5 Class Activation Map

To better understand the representative capability of CBNetV2, we visualize the class activation map (CAM) using Grad-CAM [60], which is commonly used to localize discriminative regions for image classification and object detection. As shown in Fig. 8,

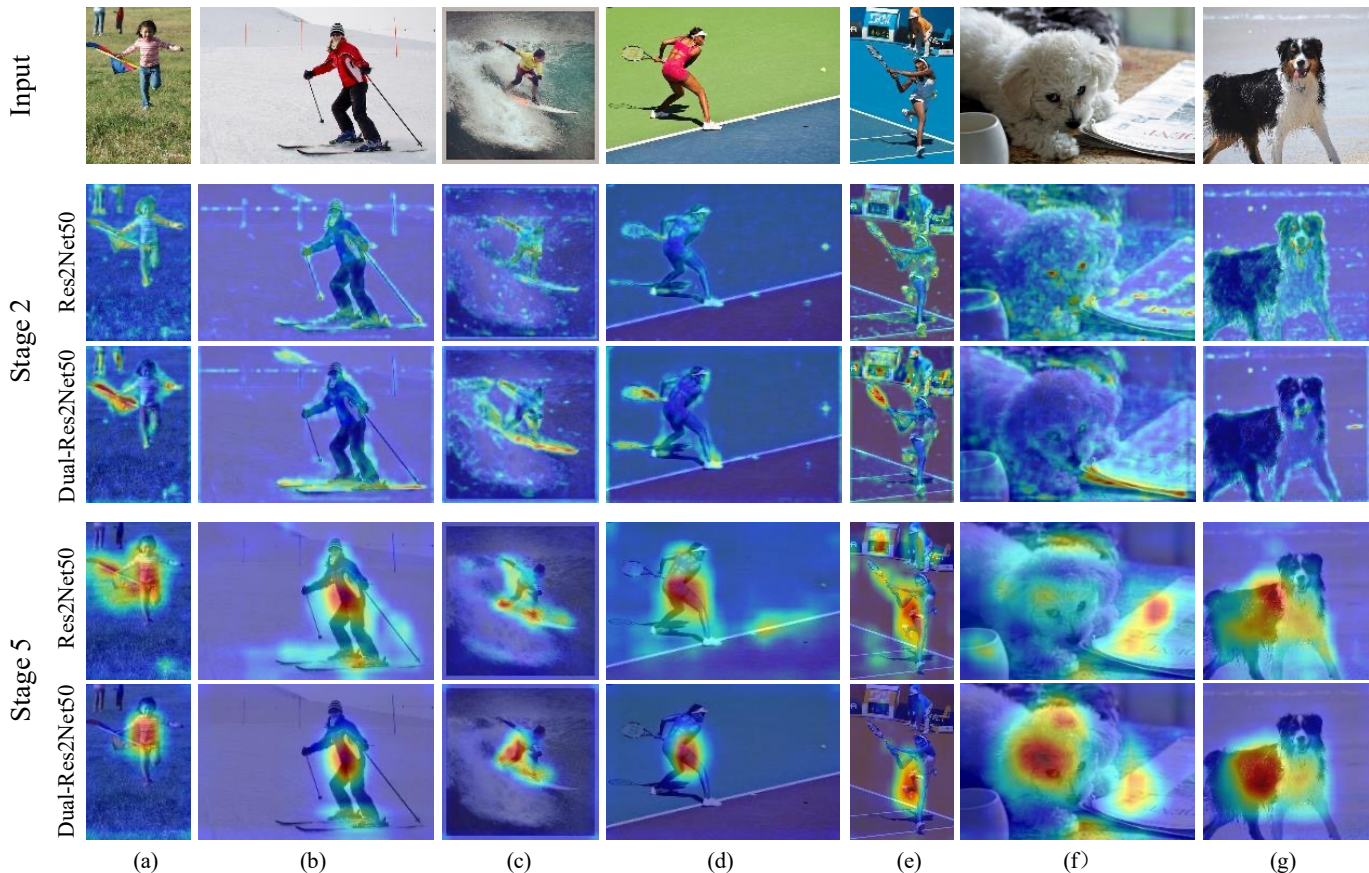


Fig. 8. Visualization comparison of the features extracted by ResNet50 and Dual-ResNet50. For each backbone, we visualize the features of the stage 2 and the stage 5 according to the size of the targets. Best viewed in color.

stronger CAM areas are covered by lighter/warmer colors. To better illustrate the multi-scale detection capability of CBNetV2, we visualize the large-scale feature maps from stage 2 (for detecting small objects) and the small-scale feature maps from stage 5 (for detecting large objects) extracted by our Dual-ResNet50 and ResNet50. Compared with ResNet, Dual-ResNet based CAM results have more concentrated activation maps on large objects of the stage 5 feature, such as the ‘person’, ‘dog’ in Fig. 8, while ResNet only partially covers the objects or is disturbed by the background. On the other hand, Dual-ResNet has a stronger ability to distinguish small objects with stage 2 feature, such as ‘kite’ in Fig. 8 (a), ‘skateboard’ in (b), ‘surfboard’ in (c), and ‘tennis racket’ in (d,e), while ResNet hardly activates on these parts.

5 CONCLUSION

In this paper, we propose a novel and flexible backbone framework, called *Composite Backbone Network V2* (CBNetV2), to improve the performance of cutting edge object detectors. CBNetV2 consists of a series of backbones with the same network architecture in parallel, the Dense Higher-Level Composition style, and the assistant supervision. Together they construct a robust representative backbone network that uses existing pre-trained backbones under the pre-training fine-tuning paradigm, which also presents a superior approach for object detection. CBNetV2 has strong generalization capabilities for different backbones and head designs of the detector architecture. Extensive experimental results demonstrate that the proposed CBNetV2 is

compatible with various backbone networks, including CNN-based (ResNet, ResNeXt, Res2Net) and Transformer-based (Swin-Transformer) ones. At the same time, CBNetV2 is more effective and efficient than simply increasing the depth and width of the network. Furthermore, CBNetV2 can be flexibly plugged into most mainstream detectors, including one-stage (*e.g.*, RetinaNet) and two-stage (Faster R-CNN, Mask R-CNN, Cascade R-CNN, and Cascade Mask R-CNN) detectors, as well as anchor-based (*e.g.*, Faster R-CNN) and anchor-free-based (ATSS) ones. Specifically, the performances of the above detectors are increased by over 3% AP. In particular, our Dual-Swin-L achieves a new record of 59.4% box AP and 51.6% mask AP on COCO *test-dev*, outperforming prior single-model single-scale results. With multi-scale testing, we achieve a new state-of-the-art result of 60.1% box AP and 52.3% mask AP without extra training data.

ACKNOWLEDGMENTS

We thank Dr. Han Hu, Prof. Ming-Ming Cheng, and Shang-Hua Gao for the insightful discussions.

REFERENCES

- [1] Y. Liu, Y. Wang, S. Wang, T. Liang, Q. Zhao, Z. Tang, and H. Ling, “Cbnet: A novel composite backbone network architecture for object detection,” in *AAAI*, 2020. 1, 2, 4, 9
- [2] A. Krizhevsky, I. Sutskever, and G. E. Hinton, “Imagenet classification with deep convolutional neural networks,” in *NeurIPS*, 2012. 1, 3
- [3] W. Liu, D. Anguelov, D. Erhan, C. Szegedy, S. E. Reed, C. Fu, and A. C. Berg, “SSD: single shot multibox detector,” in *ECCV*, 2016. 1, 2

- [4] J. Redmon, S. Divvala, R. Girshick, and A. Farhadi, "You only look once: Unified, real-time object detection," in *CVPR*, 2016. 1, 2
- [5] S. Ren, K. He, R. B. Girshick, and J. Sun, "Faster R-CNN: towards real-time object detection with region proposal networks," *TPAMI*, 2017. 1, 2
- [6] T. Lin, P. Goyal, R. B. Girshick, K. He, and P. Dollár, "Focal loss for dense object detection," *TPAMI*, 2020. 1, 2
- [7] S. Zhang, C. Chi, Y. Yao, Z. Lei, and S. Z. Li, "Bridging the gap between anchor-based and anchor-free detection via adaptive training sample selection," in *CVPR*, 2020. 1, 2, 6
- [8] K. He, G. Gkioxari, P. Dollár, and R. B. Girshick, "Mask R-CNN," in *ICCV*, 2017. 1, 2
- [9] Z. Cai and N. Vasconcelos, "Cascade R-CNN: delving into high quality object detection," in *CVPR*, 2018. 1, 2
- [10] J. Deng, W. Dong, R. Socher, L.-J. Li, K. Li, and L. Fei-Fei, "Imagenet: A large-scale hierarchical image database," in *CVPR*, 2009. 1
- [11] A. G. Howard, M. Zhu, B. Chen, D. Kalenichenko, W. Wang, T. Weyand, M. Andreetto, and H. Adam, "Mobilenets: Efficient convolutional neural networks for mobile vision applications," *arXiv preprint arXiv:1704.04861*, 2017. 1
- [12] X. Zhang, X. Zhou, M. Lin, and J. Sun, "Shufflenet: An extremely efficient convolutional neural network for mobile devices," in *CVPR*, 2018. 1
- [13] K. He, X. Zhang, S. Ren, and J. Sun, "Deep residual learning for image recognition," in *CVPR*, 2016. 1, 2, 3, 4, 5
- [14] S. Xie, R. Girshick, P. Dollár, Z. Tu, and K. He, "Aggregated residual transformations for deep neural networks," in *CVPR*, 2017. 1, 2, 3, 4
- [15] S. Gao, M. Cheng, K. Zhao, X. Zhang, M. Yang, and P. H. S. Torr, "Res2net: A new multi-scale backbone architecture," *TPAMI*, 2021. 1, 2, 3, 4
- [16] A. Vaswani, N. Shazeer, N. Parmar, J. Uszkoreit, L. Jones, A. N. Gomez, L. Kaiser, and I. Polosukhin, "Attention is all you need," in *NeurIPS*, 2017. 1, 3
- [17] Y. Li, H. Zhang, and Y. Zhang, "Rethinking training from scratch for object detection," *arXiv preprint arXiv:2106.03112*, 2021. 1
- [18] T. Lin, M. Maire, S. J. Belongie, J. Hays, P. Perona, D. Ramanan, P. Dollár, and C. L. Zitnick, "Microsoft COCO: common objects in context," in *ECCV*, 2014. 2, 5
- [19] Z. Liu, Y. Lin, Y. Cao, H. Hu, Y. Wei, Z. Zhang, S. Lin, and B. Guo, "Swin transformer: Hierarchical vision transformer using shifted windows," *arXiv preprint arXiv:2103.14030*, 2021. 2, 3, 4, 5, 6, 7
- [20] M. Liang and X. Hu, "Recurrent convolutional neural network for object recognition," in *CVPR*, 2015. 3
- [21] T. Lin, P. Dollár, R. B. Girshick, K. He, B. Hariharan, and S. J. Belongie, "Feature pyramid networks for object detection," in *CVPR*, 2017. 2, 4, 5
- [22] G. Ghiasi, T. Lin, and Q. V. Le, "NAS-FPN: learning scalable feature pyramid architecture for object detection," in *CVPR*, 2019. 2, 6
- [23] M. Tan, R. Pang, and Q. V. Le, "Efficientdet: Scalable and efficient object detection," in *CVPR*, 2020. 2, 6
- [24] J. Pang, K. Chen, J. Shi, H. Feng, W. Ouyang, and D. Lin, "Libra r-cnn: Towards balanced learning for object detection," in *CVPR*, 2019. 2
- [25] C. Zhu, Y. He, and M. Savvides, "Feature selective anchor-free module for single-shot object detection," in *CVPR*, 2019. 2, 6
- [26] Z. Tian, C. Shen, H. Chen, and T. He, "FCOS: fully convolutional one-stage object detection," in *ICCV*, 2019. 2, 6
- [27] X. Li, W. Wang, L. Wu, S. Chen, X. Hu, J. Li, J. Tang, and J. Yang, "Generalized focal loss: Learning qualified and distributed bounding boxes for dense object detection," in *NeurIPS*, 2020. 2, 6
- [28] H. Law and J. Deng, "Cornernet: Detecting objects as paired keypoints," *IJCV*, 2020. 2
- [29] K. Duan, S. Bai, L. Xie, H. Qi, Q. Huang, and Q. Tian, "Centernet: Keypoint triplets for object detection," in *ICCV*, 2019. 2
- [30] N. Wang, Y. Gao, H. Chen, P. Wang, Z. Tian, C. Shen, and Y. Zhang, "NAS-FCOS: fast neural architecture search for object detection," in *CVPR*, 2020. 2, 6
- [31] X. Du, T. Lin, P. Jin, G. Ghiasi, M. Tan, Y. Cui, Q. V. Le, and X. Song, "Spinenet: Learning scale-permuted backbone for recognition and localization," in *CVPR*, 2020. 2, 6
- [32] L. Yao, H. Xu, W. Zhang, X. Liang, and Z. Li, "SM-NAS: structural-to-modular neural architecture search for object detection," in *AAAI*, 2020. 2, 6
- [33] H. Xu, L. Yao, Z. Li, X. Liang, and W. Zhang, "Auto-fpn: Automatic network architecture adaptation for object detection beyond classification," in *ICCV*, 2019. 3, 6
- [34] Y. Chen, T. Yang, X. Zhang, G. Meng, X. Xiao, and J. Sun, "Detnas: Backbone search for object detection," in *NeurIPS*, 2019. 3
- [35] T. Liang, Y. Wang, Z. Tang, G. Hu, and H. Ling, "Opanas: One-shot path aggregation network architecture search for object detection," in *CVPR*, 2021. 3, 6
- [36] N. Carion, F. Massa, G. Synnaeve, N. Usunier, A. Kirillov, and S. Zagoryuko, "End-to-end object detection with transformers," in *ECCV*, 2020. 3, 6
- [37] K. Simonyan and A. Zisserman, "Very deep convolutional networks for large-scale image recognition," in *ICLR*, 2015. 3
- [38] G. Huang, Z. Liu, L. Van Der Maaten, and K. Q. Weinberger, "Densely connected convolutional networks," in *CVPR*, 2017. 3, 4
- [39] Z. Li, C. Peng, G. Yu, X. Zhang, Y. Deng, and J. Sun, "Detnet: Design backbone for object detection," in *ECCV*, 2018. 3
- [40] S. Sun, J. Pang, J. Shi, S. Yi, and W. Ouyang, "Fishnet: A versatile backbone for image, region, and pixel level prediction," in *NeurIPS*, 2018. 3
- [41] L. Shen, Z. Lin, and Q. Huang, "Relay backpropagation for effective learning of deep convolutional neural networks," in *ECCV*, 2016. 5
- [42] C. Szegedy, W. Liu, Y. Jia, P. Sermanet, S. E. Reed, D. Anguelov, D. Erhan, V. Vanhoucke, and A. Rabinovich, "Going deeper with convolutions," in *CVPR*, 2015. 5
- [43] C. Szegedy, V. Vanhoucke, S. Ioffe, J. Shlens, and Z. Wojna, "Rethinking the inception architecture for computer vision," in *CVPR*, 2016. 5
- [44] X. Zhu, W. Su, L. Lu, B. Li, X. Wang, and J. Dai, "Deformable detr: Deformable transformers for end-to-end object detection," in *ICLR*, 2021. 6
- [45] K. Kim and H. S. Lee, "Probabilistic anchor assignment with iou prediction for object detection," in *ECCV*, A. Vedaldi, H. Bischof, T. Brox, and J. Frahm, Eds., 2020. 6
- [46] C. Jiang, H. Xu, W. Zhang, X. Liang, and Z. Li, "SP-NAS: serial-to-parallel backbone search for object detection," in *CVPR*, 2020. 6
- [47] C.-Y. Wang, A. Bochkovskiy, and H.-Y. M. Liao, "Scaled-yolov4: Scaling cross stage partial network," in *CVPR*, 2021. 6
- [48] K. Chen, J. Wang, J. Pang, Y. Cao, Y. Xiong, X. Li, S. Sun, W. Feng, Z. Liu, J. Xu, Z. Zhang, D. Cheng, C. Zhu, T. Cheng, Q. Zhao, B. Li, X. Lu, R. Zhu, Y. Wu, J. Dai, J. Wang, J. Shi, W. Ouyang, C. C. Loy, and D. Lin, "MMDetection: Open mmlab detection toolbox and benchmark," *arXiv preprint arXiv:1906.07155*, 2019. 5, 9
- [49] K. Chen, J. Pang, J. Wang, Y. Xiong, X. Li, S. Sun, W. Feng, Z. Liu, J. Shi, W. Ouyang, C. C. Loy, and D. Lin, "Hybrid task cascade for instance segmentation," in *CVPR*, 2019. 5
- [50] N. Bodla, B. Singh, R. Chellappa, and L. S. Davis, "Soft-NMS: improving object detection with one line of code," in *ICCV*, 2017. 6
- [51] Y. Cao, J. Xu, S. Lin, F. Wei, and H. Hu, "Global context networks," *TPAMI*, 2020. 6, 7
- [52] H. Zhang, C. Wu, Z. Zhang, Y. Zhu, Z. Zhang, H. Lin, Y. Sun, T. He, J. Mueller, R. Manmatha, M. Li, and A. J. Smola, "Resnest: Split-attention networks," *arXiv preprint arXiv:2004.08955*, 2020. 6, 7
- [53] G. Ghiasi, Y. Cui, A. Srinivas, R. Qian, T. Lin, E. D. Cubuk, Q. V. Le, and B. Zoph, "Simple copy-paste is a strong data augmentation method for instance segmentation," in *CVPR*, 2021. 6, 7
- [54] Y. Wu and K. He, "Group normalization," *IJCV*, 2020. 6
- [55] H. Rezatofighi, N. Tsoi, J. Gwak, A. Sadeghian, I. D. Reid, and S. Savarese, "Generalized intersection over union: A metric and a loss for bounding box regression," in *CVPR*, 2019. 6
- [56] R. Girshick, "Fast r-cnn," in *ICCV*, 2015. 6
- [57] X. Dai, Y. Chen, B. Xiao, D. Chen, M. Liu, L. Yuan, and L. Zhang, "Dynamic head: Unifying object detection heads with attentions," in *CVPR*, 2021. 6
- [58] H. Zhang, Y. Wang, F. Dayoub, and N. Sünderhauf, "Swa object detection," *arXiv preprint arXiv:2012.12645*, 2020. 6
- [59] J. Dai, H. Qi, Y. Xiong, Y. Li, G. Zhang, H. Hu, and Y. Wei, "Deformable convolutional networks," in *ICCV*, 2017. 8
- [60] R. R. Selvaraju, M. Cogswell, A. Das, R. Vedantam, D. Parikh, and D. Batra, "Grad-cam: Visual explanations from deep networks via gradient-based localization," in *ICCV*, 2017. 9